Ethylene Carbonylation in Methanol and in Aqueous Media by Palladium(II) Catalysts Modified with 1,1′-Bis(dialkylphosphino)ferrocenes

Claudio Bianchini,* Andrea Meli, Werner Oberhauser, and Sebastien Parisel

Istituto di Chimica dei Composti Organometallici (ICCOM-CNR), Area di Ricerca CNR di Firenze, via Madonna del Piano snc, 50019 Sesto Fiorentino, Italy

Elisa Passaglia and Francesco Ciardelli

ICCOM-CNR, Sezione di Pisa, Dipartimento di Chimica e Chimica Industriale, via Risorgimento 35, 56126 Pisa, Italy

Oleg V. Gusev, Alexander M. Kal'sin, and Nikolai V. Vologdin

N. Nesmeyanov Institute of Organoelement Compounds of the Russian Academy of Sciences, Vavilov St. 28, 119991 Moscow, Russian Federation

Received November 18, 2004

Palladium(II) complexes with the formula [Pd(H_2O)(OTs)(P-P)]OTs, where P-P is 1,1′-bis(dimethylphosphino)ferrocene (dmpf), 1,1′-bis(diethylphosphino)ferrocene (depf), or 1,1′-bis(diisopropylphosphino)ferrocene (dippf), have been synthesized and used to catalyze the carbonylation of ethylene in MeOH, water, or a 1/1 water/1,4-dioxane mixture. In MeOH, the reactions catalyzed by the dmpf and depf complexes gave alternating polyketone (alt-E-CO), while methyl propanoate and 3-pentanone were selectively produced with the dippf catalyst. The last catalyst was inactive in aqueous solvent. In contrast, the dmpf and depf catalysts were active in either water or water/1,4-dioxane for the copolymerization of CO with ethylene. These two catalysts were efficient also for the terpolymerization of CO with ethylene and propene in MeOH or water/1,4-dioxane. Operando high-pressure NMR experiments and in situ reactions with model compounds have provided useful information to rationalize the activity and selectivity of the catalytic systems investigated.

Introduction

Metal complexes containing 1,1′-bis(diorganylphosphino)metallocenes are active catalysts for a variety of important catalytic reactions.[1−13] Representative examples include cross-coupling reactions,[4] the Heck reaction,[5] carbonylation of chloroarenes,[6] aryl halide amination,[7] hydroamination of alkenes,[8] glioxylate-ene reaction with chiral controllers,[9] cooligomerization of 1,3-butadiene with CO_2,[10] alternating copolymerization of CO and ethylene,[11,12] and methoxycarbonylation of styrene or ethylene.[3,11,13]

The success of 1,1′-bis(diorganylphosphino)metallocene ligands in homogeneous catalysis is largely ascribable to their excellent structural and electronic flexibility. Indeed, the coordination behavior of these ligands can be effectively tuned by an appropriate choice of the central metal (Fe, Ru, or Os) and of the substituents on either the Cp rings or the phosphorus atoms. The three

---

[1] (a) Colacot, T. J. *Platinum Met. Rev.* **2001**, *45*, 22. (b) Gan, K.-S.; Hor, T. S. A. In *Ferrocenes: Homogeneous Catalysis, Organic Synthesis, Materials Science*; Togni, A., Hayashi, T., Eds.; VCH-Wiley: Weinheim, Germany, 1995; Chapter 1.

[2] (a) Li, S.; Wei, B.; Low, P. M. N.; Lee, H. K.; Hor, T. S. A.; Xue, F.; Mak, T. C. W. *J. Chem. Soc., Dalton Trans.* **1997**, 1289. (b) Brown, J. M.; Guiry, P. J. *Inorg. Chim. Acta* **1994**, *220*, 249.

[3] Gusev, O. V.; Kal'sin, A. M.; Petrovskii, P. V.; Lyssenko, K. A.; Oprunenko, Y. F.; Bianchini, C.; Meli, A.; Oberhauser, W. *Organometallics* **2003**, *22*, 913.

[4] (a) Ogasawara, M.; Yoshida, K.; Hayashi, T. *Organometallics* **2000**, *19*, 1567. (b) Bosch, B. E.; Brümmer, I.; Kunz, K.; Erker, G.; Frölich, R.; Kotila, S. *Organometallics* **2000**, *19*, 1255. (c) Xie, Y.: Tan, G. K.; Yan, Y. K.; Vittal, J. J.; Ng, S. C.; Hor, T. S. A. *J. Chem. Soc., Dalton Trans.* **1999**, 773. (d) Fong, S.-W. A.; Hor, T. S. A. *J. Cluster Sci.* **1998**, *9*, 351. (e) Hayashi, T.; Konishi, M.; Kobori, Y.; Kumada, M.; Higuchi, T.; Hirotsu, K. *J. Am. Chem. Soc.* **1984**, *106*, 158.

[5] (a) Jutand, A.; Hii, K.-K.; Thornton-Pett, M.; Brown, J. M. *Organometallics* **1999**, *18*, 5367. (b) Boyes, A. L.; Butler, I. R.; Quayle, S. C. *Tetrahedron Lett.* **1998**, *39*, 7763. (c) Brown, J. M.; Hii, K.-K. *Angew. Chem., Int. Ed. Engl.* **1996**, *35*, 657.

[6] Mägerlein, W.; Indolese, A. F.; Beller, M. *Angew. Chem., Int. Ed.* **2001**, *40*, 2856.

[7] (a) Hartwig, J. F. *Angew. Chem., Int. Ed.* **1998**, *37*, 2090. (b) Hartwig, J. F. *Acc. Chem. Res.* **1998**, *31*, 852. (c) Driver, M. S.; Hartwig, J. F. *J. Am. Chem. Soc.* **1996**, *118*, 7217.

[8] (a) Li, K.; Horton, P. N.; Hursthouse, M. B.; Hii, K.-K. *J. Organomet. Chem.* **2003**, *665*, 250. (b) Müller, T. E.; Berger, M.; Grosche, M.; Herdtweck, E.; Schmidtchen, F. P. *Organometallics* **2001**, *20*, 4384.

[9] Mikami, K.; Aikawa, K. *Org. Lett.* **2002**, *4*, 99.

[10] Elsagir, A. R.; Gassner, F.; Görls, H.; Dinjus, E. *J. Organomet. Chem.* **2000**, *597*, 139.

[11] (a) Bianchini, C.; Meli, A.; Oberhauser, W.; van Leeuwen, P. W. N. M.; Zuideveld, M. A.; Freixa, Z.; Kamer, P. C. J.; Spek, A. L.; Gusev, O. V.; Kal'sin, A. M. *Organometallics* **2003**, *22*, 2409. (b) Gusev, O. V.; Kal'sin, A. M.; Peterleitner, M. G.; Petrovskii, P. V.; Lyssenko, K. A.; Akhmedov, N. G.; Bianchini, C.; Meli, A.; Oberhauser, W. *Organometallics* **2002**, *21*, 3637.

[12] Zuideveld, M. A.; Kamer, P. C. J.; van Leeuwen, P. W. N. M.; Klusener, P. A. A.; Stil, H. A.; Roobeek, C. F. *J. Am. Chem. Soc.* **1998**, *120*, 7977.

[13] Bianchini, C.; Meli, A.; Oberhauser, W.; Parisel, S.; Gusev, O. V.; Kal'sin, A. M.; Vologdin, N. V.; Dolgushin, F. M. *J. Mol. Catal. A* **2004**, *224*, 35.

10.1021/om049109w CCC: $30.25

Chart 1

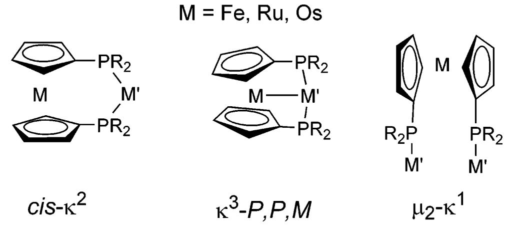

major coordination modes in isolated complexes are *cis*-κ^2-*P,P*,[2,3,5,10–18] κ^3-*P,P,M*,[3,11,13,17,18] and μ_2-κ^1-*P*,[18b,19,20] while the plain unidentate (κ^1) bonding is often invoked for transient species (Chart 1).

In the vast majority of 1,1′-bis(diorganylphosphino)metallocene ligands employed in catalysis the phosphorus atoms contain aryl groups, generally phenyls. Recently, however, much interest has been focused on ligands bearing P(alkyl)$_2$ groups.[5b,8a,10,15,16,18] Besides increasing the basicity of the phosphorus donors,[21] alkyl substituents have proved more amenable than aryl substituents to control the steric hindrance at the P−M′-P grouping, which, in turn, is a key factor to switch the coordination mode from *cis*-κ^2-*P,P* to κ^3-*P,P,M* with remarkable effects on the chemical reactivity.[3,11,13,18] Another peculiar aspect of 1,1′-bis(dialkylphosphino)metallocenes is their capability to form water-soluble metal complexes with no need of polar groups incorporated into the ligand skeleton, as is required for classical chelating diphosphines such as dppp and dppe.[22] However, the use of bis(dialkylphosphino)metallocene metal complexes in aqueous catalysis seems to have no precedent in the relevant literature.

The aim of this paper is to provide unprecedented information on the catalytic behavior of palladium(II) precursors modified with 1,1′-bis(dialkylphosphino)ferrocene ligands, with particular attention to processes performed in aqueous media. The reaction investigated is the carbonylation of either ethylene or ethylene−propene mixtures in the typical MeOH solvent as well as in aqueous solvents such as water and water/1,4-dioxane. Indeed, over the last 5 years, palladium(II) complexes with 1,1′-bis(diarylphosphino)metallocene ligands have been extensively used both as effective catalysts for the carbonylation of ethylene and as model compounds to study this relevant reaction.[3,11,12,18c] The catalytic performance of such complexes is strictly controlled by the nature of both the metallocene metal (Fe, Ru, Os) and the substituents on the Cp rings, to the extent that a variation of either parameter may result in the selective formation of a variety of products spanning from alternating polyketones (alt-E-CO) to low-molecular-weight esters, diesters, and ketones (Scheme 1).[3,11,12]

Scheme 1

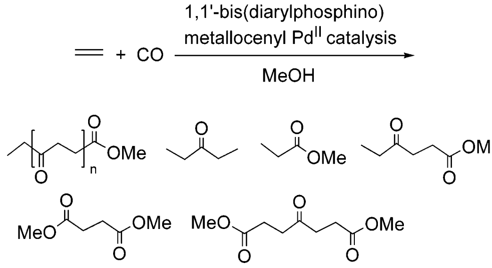

Chart 2

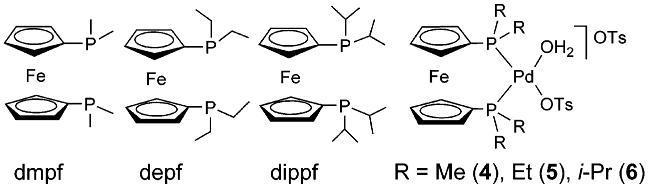

The ligands and the palladium complexes employed as catalyst precursors in this study are illustrated in Chart 2.

Experimental Section

General Procedures. All reactions and manipulations were carried out under an atmosphere of nitrogen using Schlenk-type techniques. All reagents and solvents were used as purchased from commercial suppliers. The compounds 1,1′-bis(dimethylphosphino)ferrocene (dmpf),[23] bis(diethylphosphino)ferrocene (depf),[24] bis(diisopropylphosphino)ferrocene (dippf),[10] PdCl(Me)(COD) (COD = cycloocta-1,5-diene),[25] PdCl$_2$(dippf)[10] (**3**), PdCl(Me)(depf)[18b] (**9**), and PdCl(Me)(dippf)[15] (**10**) were synthesized according to published procedures. Carbonylation reactions were performed with a 325 mL stainless steel autoclave, constructed at the ICCOM-CNR (Firenze, Italy), equipped with a magnetic drive stirrer and a Parr 4842 temperature and pressure controller. The autoclave was connected to a gas reservoir to maintain a constant pressure over all the catalytic reactions. Deuterated solvents for NMR

---

(14) (a) Butler, I. R.; Cullen, W. R.; Kim, T.-J.; Rettig, S. J.; Trotter, J. *Organometallics* **1985**, *4*, 972. (b) Stang, P. J.; Olenyuk, B.; Fan, J.; Arif, A. M. *Organometallics* **1996**, *15*, 904. (c) Corain, B.; Longato, B.; Favero, G.; Ajo, D.; Pilloni, G.; Russo, U.; Creissl, F. R. *Inorg. Chim. Acta* **1989**, *157*, 259. (d) Vasapollo, G.; Toniolo, L.; Cavinato, G.; Bigoli, F.; Lanfranchi, M.; Pellinghelli, M. A. *J. Organomet. Chem.* **1994**, *481*, 173. (e) Dekker, G. P. C. M.; Elsevier, C. J.; Vrieze, K.; van Leeuwen, P. W. N. M. *Organometallics* **1992**, *11*, 1598. (f) Longato, B.; Pilloni, G.; Valle, G.; Corain, B. *Inorg. Chem.* **1988**, *27*, 956. (g) Fang, Z.-G.; Low, P. M. N.; Ng, S.-C.; Hor, T. S. A. *J. Organomet. Chem.* **1994**, *483*, 17. (h) Li, G.; Tan, A. L.; Yip, W.-H.; Mak, T. C. W.; Hor, T. S. A. *J. Chem. Soc., Dalton Trans.* **1996**, 4315.

(15) Li, K.; Guzei, I. A.; Darkwa, J. *Polyhedron* **2003**, *22*, 805.

(16) Kiso, Y.; Kumada, M.; Tamao, K.; Umeno, M. *J. Organomet. Chem.* **1973**, *50*, 297.

(17) Sato, M.; Shigeta, H.; Sekino, M.; Akabori, S. *J. Organomet. Chem.* **1993**, *458*, 199.

(18) (a) Zuideveld, M. A.; Swennenhuis, B. H. G.; Kamer, P. C. J.; van Leeuwen, P. W. N. M. *J. Organomet. Chem.* **2001**, *637*, 805. (b) Zuideveld, M. A.; Swennenhuis, B. H. G.; Boele, M. D. K.; Guari, Y.; van Strijdonck, G. P. F.; Reek, J. N. H.; Kamer, P. C. J.; Goubitz, K.; Fraanje, J.; Lutz, M.; Spek, A. L.; van Leeuwen, P. W. N. M. *Dalton* **2002**, 2308. (c) van Leeuwen, P. W. N. M.; Zuideveld, M. A.; Swennenhuis, B. H. G.; Freixa, Z.; Kamer, P. C. J.; Goubitz, K.; Fraanje, J.; Lutz, M.; Spek, A. L. *J. Am. Chem. Soc.* **2003**, *125*, 5523.

(19) (a) Hor, T. S. A.; Neo, S. P.; Tan, C. S.; Mak, T. C. W.; Leung, K. W. P.; Wang, R.-J. *Inorg. Chem.* **1992**, *31*, 4510. (b) Yan, Y. K.; Chan, H. S. O.; Hor, T. S. A.; Tan, K.-L.; Liu, L.-K.; Wen, Y.-S. *J. Chem. Soc., Dalton Trans.* **1992**, 423.

(20) (a) Unruh, J. D.; Christenson, J. R. *J. Mol. Catal.* **1982**, *14*, 19. (b) Casellato, U.; Corain, B.; Graziani, R.; Longato, B.; Pilloni, G. *Inorg. Chem.* **1990**, *29*, 1193. (c) Viotte, M.; Gautheron, B.; Kubicki, M. M.; Mugnier, Y.; Parish, R. V. *Inorg. Chem.* **1995**, *34*, 3465.

(21) (a) O'Connor, A. R.; Nataro, C. *Organometallics* **2004**, *23*, 615. (b) Tolman, C. A. *J. Am. Chem. Soc.* **1970**, *92*, 2953. (c) McAuliffe, C. In *Comprehensive Coordination Chemistry*; Wilkinson, G., Gillard, R. D., McCleverty, J., Eds.; Pergamon: Oxford, U.K., 1987; Vol. 2, pp 1030−1033.

(22) Bianchini, C.; Meli, A. *Coord. Chem. Rev.* **2002**, *225*, 35.

(23) (a) Bishop, J. J.; Davison, A.; Katcher, M. L.; Lichtenberg, D. W.; Merrill, R. E.; Smart, J. C. *J. Organomet. Chem.* **1971**, *27*, 241. (b) Kumada, M.; Kiso, Y.; Umeno, M. *Chem. Commun.* **1970**, 611.

(24) Butler, I. R.; Cullen, W. R.; Kim, T.-J. *Synth. React. Inorg. Met.-Org. Chem.* **1985**, *15*, 109.

(25) (a) Drew, D.; Doyle, J. R. *Inorg. Synth.* **1972**, *13*, 47. (b) Rülke, R. E.; Ernsting, J. M.; Spek, A. L.; Elsevier, C. J.; van Leeuwen, P. W. N. M.; Vrieze, K. *Inorg. Chem.* **1993**, *32*, 5769.

measurements were dried over molecular sieves. ^{1}H, ^{13}C{^{1}H}, and ^{31}P{^{1}H} NMR spectra were routinely obtained on a Bruker ACP 200 spectrometer (200.13, 50.32, and 81.01 MHz, respectively). ^{1}H and ^{13}C{^{1}H} NMR spectra of both polymer materials and selected complexes were recorded on a Bruker AMX 400 spectrometer (400.13 and 100.61 MHz, respectively). Chemical shifts are reported in ppm (δ) with reference to either TMS as an internal standard (^{1}H and ^{13}C{^{1}H} NMR spectra) or 85% H_3PO_4 as an external standard (^{31}P{^{1}H} NMR spectra). The 10 mm sapphire NMR tube was purchased from Saphikon, Milford, NH, while the titanium high-pressure charging head was constructed at the ICCOM-CNR (Firenze, Italy).[26] *Caution! Since high gas pressures are involved, safety precautions must be taken at all stages of studies involving high-pressure NMR tubes*. Infrared spectra were recorded on a Perkin-Elmer Spectrum BX FT-IR spectrophotometer; a cell with KBr windows and 0.2 mm spacer between the KBr plates was employed for solution measurements. Elemental analyses were performed using a Carlo Erba Model 106 elemental analyzer. Conductivities were measured with an ORION Model 990101 conductance cell connected to a Model 101 conductivity meter. The conductivity data[27] were obtained at sample concentrations of ca. 10^{-3} M in nitroethane solutions. Melting points were recorded on a Electrothermal IA 9000 Series digital melting point apparatus. DSC analyses were performed at 5 and 20 °C min^{-1} on a Perkin-Elmer Series 7 instrument calibrated with In and Zn standards. TGA analyses were obtained under nitrogen (60 mL min^{-1}) with a TGA Mettler Toledo instrument at 10 °C min^{-1}. GC analyses were performed on a Shimadzu GC-14 A gas chromatograph equipped with a flame ionization detector and a 30 m (0.25 mm i.d., 0.25 μm film thickness) SPB-1 Supelco fused silica capillary column. The product composition of the catalytic reactions was determined by using 1,2-dimethoxyethane as the internal standard. GC/MS analyses were performed on a Shimadzu QP 5000 apparatus equipped with a column identical with that used for GC analysis.

Catalytic Carbonylation of Ethylene and Ethylene/Propene in Methanol, Water, and 1/1 (v/v) Water/1,4-Dioxane. Typically, a solution of the precatalyst (0.01 mmol) in 100 mL of the appropriate solvent was introduced by suction into a 325 mL autoclave, previously evacuated by a vacuum pump, containing, if required, solid samples of benzoquinone (BQ) and/or *p*-toluenesulfonic acid monohydrate (TsOH). The desired amount of propene was charged by cooling the autoclave with an ice/acetone bath. The autoclave was then charged with 1/1 CO/ethylene (30 bar) at room temperature and heated to 85 °C. As soon as the temperature was reached, stirring was applied (1400 rpm) and the autoclave was connected to a CO/ethylene reservoir to maintain a constant pressure of 40 bar during the experiment. After the desired reaction time (1−3 h), the autoclave was disconnected from the gas reservoir and cooled to 10 °C by means of an ice/acetone cooling bath. Afterward, the pressure was released from the autoclave and the polymer, if any, was filtered off, washed with methanol, and dried to a constant weight at 50 °C under vacuum. Alternatively, the solution was analyzed by GC.

Synthesis of $PdCl_2$(dmpf) (1) and $PdCl_2$(depf) (2). These orange complexes were synthesized in 80−90% yield by reaction of the appropriate diphosphine ligand with $PdCl_2$(COD) in CH_2Cl_2. Crystals of **1** suitable for a single-crystal diffraction analysis were obtained by concentrating a CH_2Cl_2 solution of **1** at room temperature.

1. Anal. Calcd for $C_{14}H_{20}Cl_2FeP_2Pd$: C, 34.78; H, 4.17. Found: C, 34.71; H, 4.12. ^{1}H NMR ($CDCl_3$): δ 2.06 (d, *J*(HP) = 10.3 Hz, 12H, Me), 4.50 (s, 8H, H Cp). ^{31}P{^{1}H} NMR ($CDCl_3$) δ 15.4 (s).[16]

2. Anal. Calcd for $C_{18}H_{28}Cl_2FeP_2Pd$: C, 40.07; H, 5.23. Found: C, 39.99; H, 5.22. ^{1}H NMR ($CDCl_3$): δ 1.33 (br s, 12H, CH$_2$C*H$_3$*), 2.19 (br s, 4H, C*H*HCH$_3$), 2.50 (br s, 4H, CH*H*CH$_3$), 4.49 (br s, 4H, β-H Cp), 4.52 (br s, 4H, α-H Cp). ^{31}P{^{1}H} NMR ($CDCl_3$): δ 42.8 (s).

Synthesis of [Pd(OTs)(H_2O)(dmpf)]OTs (4), [Pd(OTs)(H_2O)(depf)]OTs (5), and [Pd(OTs)(H_2O)(dippf)]OTs (6). Solid silver tosylate (1.17 mmol) was added to the orange solution of $PdCl_2$(P-P) (0.56 mmol) in CH_2Cl_2 (50 mL) at room temperature under nitrogen. The resulting suspension was stirred for 2 h at room temperature and then filtered through a column of Celite. The deep red filtrate was concentrated to ca. 5 mL, and then deaerated diethyl ether was added to precipitate the red product, which was filtered off, washed with diethyl ether, and dried under a stream of nitrogen. The yields ranged from 70 to 85%.

4. Crystals suitable for X-ray analysis were obtained by recrystallization from CH_2Cl_2 and toluene. Anal. Calcd for $C_{28}H_{36}FeO_7P_2PdS_2$: C, 43.51; H, 4.69. Found: C, 43.45; H, 4.64. Λ_M (nitroethane) = 16 Ω^{-1} cm^2 mol^{-1}. ^{1}H NMR ($CDCl_3$): δ 1.99 (d, *J*(HP) = 12.7 Hz, 12H, Me), 2.32 (s, 6H, Me OTs), 4.10 (br s, 2H, H_2O), 4.49 (br s, 4H, β-H Cp), 5.02 (br s, 4H, α-H Cp), 7.07 (br s, 4H, H OTs), 7.76 (br s, 4H, H OTs). ^{13}C{^{1}H} NMR (CD_2Cl_2): δ 17.30 (s, Me), 21.73 (s, Me OTs), 74.10 (t, *J*(CP) = 3.9 Hz, β-C Cp), 75.06 (t, *J*(CP) = 6.2 Hz, α-C Cp), 77.70 (m, $|^1J(CP) + {}^2J(CP)|$ = 68.3 Hz, ipso-C Cp), 126.90 (s, CH OTs), 129.48 (s, CH OTs), 141.40 (s, C OTs), 142.10 (s, C OTs). ^{31}P{^{1}H} NMR ($CDCl_3$): δ 30.4 (s).

5. Anal. Calcd for $C_{32}H_{44}FeO_7P_2PdS_2$: C, 46.36; H, 5.35. Found: C, 46.24; H, 5.29. Λ_M (nitroethane) = 17 Ω^{-1} cm^2 mol^{-1}. ^{1}H NMR (CD_2Cl_2, 400.13 MHz): δ 1.26 (dt, *J*(HP) = 19.1 Hz, *J*(HH) = 7.6 Hz, 12H, CH$_2$C*H$_3$*), 2.34 (m, 4H, C*H*HCH$_3$), 2.38 (m, 4H, CH*H*CH$_3$), 2.38 (s, 6H, Me OTs), 4.57 (m, 4H, β-H Cp), 5.10 (m, 4H, α-H Cp), 5.72 (br s, 2H, H_2O), 7.12 (d, *J*(HH) = 7.8 Hz, 4H, H OTs), 7.72 (d, *J*(HH) = 7.8 Hz, 4H, H OTs). ^{13}C{^{1}H} NMR (CD_2Cl_2, 100.61 MHz): δ 7.81 (s, CH$_2$CH$_3$), 19.16 (d, *J*(CP) = 33.4 Hz, *C*H$_2$CH$_3$), 20.87 (s, Me OTs), 72.43 (t, *J*(CP) = 3.9 Hz, β-C Cp), 74.05 (t, *J*(CP) = 4.9 Hz, α-C Cp), 74.07 (m, $|^1J(CP) + {}^2J(CP)|$ = 64.5 Hz, ipso-C Cp), 124.97 (s, CH OTs), 127.41 (s, CH OTs), 139.12 (s, C OTs), 140.06 (s, C OTs). ^{31}P{^{1}H} NMR ($CDCl_3$): δ 53.4 (s).

6. Anal. Calcd for $C_{36}H_{52}FeO_7P_2PdS_2$: C, 48.85; H, 5.92. Found: C, 48.74; H, 5.89. Λ_M (nitroethane) = 15 Ω^{-1} cm^2 mol^{-1}. ^{1}H NMR ($CDCl_3$): δ 1.34 (dd, *J*(HP) = 17.7 Hz, *J*(HH) = 7.2 Hz, 12H, CH*Me*Me), 1.67 (dd, *J*(HP) = 17.7 Hz, *J*(HH) = 7.2 Hz, 12H, CHMe*Me*), 2.31 (s, 6H, Me OTs), 2.66 (m, 4H, C*H*MeMe), 4.25 (br s, 2H, H_2O), 4.58 (br s, 4H, β-H Cp), 4.97 (br s, 4H, α-H Cp), 7.06 (d, *J*(HH) = 7.8 Hz, 4H, H OTs), 7.69 (d, *J*(HH) = 7.8 Hz, 4H, H OTs). ^{13}C{^{1}H} NMR ($CDCl_3$): δ 19.77 (s, CH*Me*Me), 20.72 (s, CHMe*Me*), 21.68 (s, Me OTs), 28.32 (m, *C*HMeMe), 72.92 (m, $|^1J(CP) + {}^2J(CP)|$ = 56.6 Hz, ipso-C Cp), 73.76 (t, *J*(CP) = 3.5 Hz, β-C Cp), 75.54 (t, *J*(CP) = 5.5 Hz, α-C Cp), 126.49 (s, CH OTs), 129.09 (s, CH OTs), 140.51 (s, C OTs), 141.75 (s, C OTs). ^{31}P{^{1}H} NMR ($CDCl_3$): δ 82.9 (s).

Compounds **4**−**6** are soluble in polar organic solvents as well as in water, where concentrations of 48, 21, and 11 mg/mL can be obtained, respectively.

Synthesis of [PdCl(Me)(dmpf)]$_2$ (7). A solution of PdCl(Me)(COD) (106 mg, 0.40 mmol) and dmpf (128 mg, 0.42 mmol) in benzene (10 mL) was stirred for 2 h at room temperature under nitrogen. Portionwise addition of diethyl ether (10 mL) led to the precipitation of the product, which was filtered off and dried under a stream of nitrogen; yield 85%. Anal. Calcd for $C_{30}H_{46}Cl_2Fe_2P_4Pd_2$: C, 38.91; H, 5.01. Found: C, 38.85; H, 4.99. ^{1}H NMR (CD_2Cl_2): δ 0.56 (t, *J*(HP) = 6.5 Hz, 6H, Pd−Me), 1.49 (br s, 12H, Me), 1.74 (br s, 12H, Me), 4.53 (br s, 8H, β-H Cp), 5.17 (br s, 8H, α-H Cp). ^{31}P{^{1}H} NMR (CD_2Cl_2): δ −10.0 (s).

Synthesis of PdCl(Me)(dmpf) (8). A solution of **7** (40 mg, 0.04 mmol) in CH_2Cl_2 (20 mL) was refluxed under nitrogen

---

[26] Bianchini, C.; Meli, A.; Traversi, A. Ital. Patent FI A000025, 1997.

[27] (a) Geary, W. J. *Coord. Chem. Rev*. **1971**, *7*, 81. (b) Morassi, R.; Sacconi, L. *J. Chem. Soc. A* **1971**, 492.

for 30 min. Afterward, the solution was concentrated to half of the original volume and 20 mL of *n*-pentane was added to complete the precipitation of the orange product, which was filtered off and dried under a stream of nitrogen. Yield: 85%. Anal. Calcd for $C_{15}H_{23}ClFeP_2Pd$: C, 38.91; H, 5.01. Found: C, 38.78; H, 4.95. ^1H NMR (CD_2Cl_2): δ 0.66 (dd, *J*(HP) = 4.5 Hz, *J*(HP) = 8.1 Hz, 3H, Pd−Me), 1.63 (d, *J*(HP) = 7.9 Hz, 6H, Me), 1.64 (d, *J*(HP) = 10.0 Hz, 6H, Me), 4.34−4.41 (m, 8H, Cp). $^{31}P\{^1H\}$ NMR (CD_2Cl_2): δ 3.2 (d, *J*(PP) = 29.8 Hz), −12.8 (d).

Synthesis of [Pd(Me)(MeCN)(P-P)]B(Ar′)$_4$ (P-P = dmpf (11), depf (12), dippf (13)). MeCN (300 μL) and NaB(Ar′)$_4$ (Ar′ = 3,5-bis(trifluoromethyl)phenyl, 55 mg, 0.06 mmol) were added in sequence to a solution of the appropriate chloro methyl derivate **8**−**10** (0.06 mmol) in CH_2Cl_2 (10 mL) at room temperature under nitrogen. The suspension was stirred for 10 min and then filtered through a column of Celite to remove the formed NaCl. The filtrate was concentrated to dryness, and the orange residue was washed with diethyl ether and collected by filtration; yield 80−90%.

11. Anal. Calcd for $C_{49}H_{38}BF_{24}FeNP_2Pd$: C, 44.19; H, 2.87. Found: C, 44.15; H, 2.85. ^1H NMR (CD_2Cl_2): δ 0.67 (dd, *J*(HP) = 7.4 Hz, *J*(HP) = 3.3 Hz, 3H, Pd−Me), 1.57 (d, *J*(HP) = 7.6 Hz, 6H, Me), 1.66 (d, *J*(HP) = 10.6 Hz, 6H, Me), 2.08 (s, 3H, MeCN), 4.48 (br s, 8H, Cp), 7.59 (br s, 4H, *p*-aryl), 7.75 (br s, 8H, *o*-aryl). $^{31}P\{^1H\}$ NMR (CD_2Cl_2): δ 6.1 (d, *J*(PP) = 33.0 Hz), −13.7 (d).

12. Anal. Calcd for $C_{53}H_{46}BF_{24}FeNP_2Pd$: C, 45.88; H, 3.31. Found: C, 45.45; H, 3.10. ^1H NMR (CD_2Cl_2): δ 0.67 (dd, *J*(HP) = 7.2 Hz, *J*(HP) = 3.2 Hz, 3H, Pd−Me), 1.11 (t, *J*(HH) = 8.0 Hz, 6H, CH_2CH_3), 1.20 (t, *J*(HH) = 8.6 Hz, 6H, CH_2CH_3), 1.92 (m, 8H, CH_2CH_3), 2.12 (s, 3H, MeCN), 4.39−4.49 (m, 8H, Cp), 7.58 (br s, 4H, *p*-aryl), 7.74 (br s, 8H, *o*-aryl). $^{31}P\{^1H\}$ NMR (CD_2Cl_2): δ 32.6 (d, *J*(PP) = 29.1 Hz), 9.3.

13. Anal. Calcd for $C_{57}H_{54}BF_{24}FeNP_2Pd$: C, 47.43; H, 3.74. Found: C, 47.30; H, 3.50. ^1H NMR (CD_2Cl_2): δ 0.77 (dd, *J*(HP) = 6.5, 2.2 Hz, 3H, Pd−Me), 1.15 (m, 12H, CHMe*Me*), 1.30 (m, 12H, CH*Me*Me), 2.10 (s, 3H, MeCN), 2.30 (m, 2H, C*H*Me$_2$), 2.51 (m, 2H, C*H*Me$_2$), 4.38 (s, 2H, Cp), 4.45 (s, 2H, Cp), 4.50 (s, 4H, Cp), 7.58 (br s, 4H, *p*-aryl), 7.74 (br s, 8H, *o*-aryl). $^{31}P\{^1H\}$ NMR (CD_2Cl_2): δ 55.1 (d, *J*(PP) = 21.0 Hz), 33.1.

Carbonylation of the Methyl Acetonitrile Complexes 11−13. In Situ NMR Synthesis of the Acetyl Complexes [Pd(MeCN)(C(O)Me)(P-P)]B(Ar′)$_4$ (P-P = dmpf (14), depf (15)) and [Pd(C(O)Me)(dippf)]B(Ar′)$_4$ (16). CO was bubbled through the orange solution of the appropriate methyl acetonitrile complex **11**−**13** (0.03 mmol) in CD_2Cl_2 (1.5 mL) at −20 °C for 5 min. Afterward, the solution was purged with a stream of nitrogen for 1 min and transferred into a 5 mm NMR tube at −20 °C. $^{31}P\{^1H\}$ and ^1H NMR spectra recorded at room temperature showed the quantitative conversion of **11**−**13** into **14**−**16**. Better resolution of the ^1H NMR spectra was obtained by acquiring the spectra at lower temperatures (−40 °C for **14** and −10 °C for **15**).

Parallel experiments were carried out in CH_2Cl_2, and the final solutions were analyzed by IR spectroscopy.

14. ^1H NMR (CD_2Cl_2, −40 °C): δ 1.46 (d, *J*(HP) = 6.0 Hz, 6H, Me), 1.50 (d, 6H, *J*(HP) = 8.8 Hz, Me), 2.06 (s, 3H, MeCN), 2.50 (br s, 3H, C(O)Me), 4.40 (br s, 4H, H Cp), 4.45 (br s, 4H, H Cp), 7.58 (br s, 4H, *p*-aryl), 7.74 (br s, 8H, *o*-aryl). $^{31}P\{^1H\}$ NMR (CD_2Cl_2, −40 °C): δ −2.2 (d, *J*(PP) = 59.0 Hz), −17.5 (d). IR (CH_2Cl_2): ν(CO) 1694 cm^{-1}.

15. ^1H NMR (CD_2Cl_2, −10 °C): δ 1.03 (t, *J*(HH) = 7.8 Hz, 6H, CH_2CH_3), 1.11 (t, *J*(HH) = 7.8 Hz, 6H, CH_2CH_3), 1.81 (m, 8H, CH_2CH_3), 2.09 (s, 3H, MeCN), 2.52 (s, 3H, C(O)Me), 4.40−4.51 (m, 8H, Cp), 7.58 (br s, 4H, *p*-aryl), 7.73 (br s, 8H, *o*-aryl). $^{31}P\{^1H\}$ NMR (CD_2Cl_2, −10 °C): δ 19.9 (d, *J*(PP) = 57.0 Hz), 5.1 (d). IR (CH_2Cl_2): ν(CO) 1694 cm^{-1}.

16. ^1H NMR (CD_2Cl_2, 20 °C): δ 1.29 (m, 24H, CH*Me*Me), 2.39 (m, 4H, C*H*MeMe), 2.81 (s, 3H, C(O)Me), 4.22 (br s, 4H, H Cp), 4.89 (br s, 4H, H Cp), 7.58 (br s, 4H, *p*-aryl), 7.73 (br s, 8H, *o*-aryl). $^{31}P\{^1H\}$ NMR (CD_2Cl_2, 20 °C): δ 15.4 (s). IR (CH_2Cl_2): ν(CO) 1698 cm^{-1}.

Reaction of the Acetyl Complexes 14−16 with Ethylene. In Situ NMR Synthesis of the β-Chelate Derivatives [Pd(CH$_2$CH$_2$C(O)Me)(P-P)]B(Ar′)$_4$ (P-P = dmpf (17), depf (18), dippf (19)). Typically, a solution of an acetyl complex (0.03 mmol) in CD_2Cl_2 (1.5 mL), prepared in situ as reported above under nitrogen at −20 °C, was saturated with ethylene. $^{31}P\{^1H\}$ and ^1H NMR spectra recorded at −20 °C showed the quantitative formation of the β-chelate. Parallel experiments were carried out in CH_2Cl_2, and the final solutions were analyzed by IR spectroscopy. Given the selectivity of the reactions, no attempt was made to isolate the β-chelates, and their solutions were straightforwardly employed for further reactivity studies.

17. ^1H NMR (CD_2Cl_2, −20 °C): δ 1.63 (d, *J*(HP) = 8.2 Hz, 6H, Me), 1.64 (d, *J*(HP) = 11.2 Hz, 6H, Me), 1.81 (m, 2H, Pd−CH$_2$), 2.39 (s, 3H, C(O)Me), 3.21 (dt, *J*(HP) = 15.0 Hz, *J*(HH) = 6.3 Hz, 2H, *CH$_2$*C(O)Me), 4.50 (br s, 8H, Cp), 7.59 (br s, 4H, *p*-aryl), 7.75 (br s, 8H, *o*-aryl). $^{31}P\{^1H\}$ NMR (CD_2Cl_2, −20 °C): δ 7.4 (d, *J*(PP) = 35.7 Hz), −9.8 (d). IR (CH_2Cl_2): ν(CO) 1632 cm^{-1}.

18. ^1H NMR (CD_2Cl_2, −20 °C): δ 1.10 (m, 12H, CH_2CH_3), 1.70 (dt, *J*(HP) = 6.0 Hz, *J*(HH) = 2.3 Hz, 2H, Pd−CH$_2$), 1.90 (m, 8H, CH_2CH_3), 2.40 (s, 3H, C(O)Me), 3.12 (dt, *J* = 9.1 Hz, *J* = 6.2 Hz, 2H, CH$_2$CO), 4.45 (br s, 8H, Cp), 7.56 (br s, 4H, *p*-aryl), 7.75 (br s, 8H, *o*-aryl). $^{31}P\{^1H\}$ NMR (CD_2Cl_2, −20 °C): δ 31.8 (d, *J*(PP) = 33.6 Hz), 12.1 (d). IR (CH_2Cl_2): ν(CO) 1633 cm^{-1}.

19. Better resolution of the ^1H NMR spectrum was obtained at 0 °C. ^1H NMR (CD_2Cl_2, 0 °C): δ 1.25 (m, 24H, CH*Me*$_2$), 1.89 (dt, *J*(HP) = 6.0 Hz, *J*(HH) = 2.3 Hz, 2H, Pd−CH$_2$), 2.31 (m, 4H, C*H*Me$_2$), 2.44 (s, 3H, C(O)Me), 3.12 (dt, *J*(HP) = 9.1 Hz, *J*(HH) = 6.2 Hz, 2H, *CH$_2$*C(O)Me), 4.48 (br s, 8H, Cp), 7.58 (br s, 4H, *p*-aryl), 7.75 (br s, 8H, *o*-aryl). $^{31}P\{^1H\}$ NMR (CD_2Cl_2, −20 °C): δ 57.9 (d, *J*(PP) = 23.6 Hz), 34.9 (d). IR (CH_2Cl_2): ν(CO) 1634 cm^{-1}.

Reaction of the β-Chelate Complexes 17−19 with Water. In Situ NMR and IR Experiments. A solution of the appropriate β-chelate (0.03 mmol) in CD_2Cl_2 (1.5 mL) was prepared in situ as reported above at −20 °C under ethylene and then transferred into a 5 mm NMR tube equipped with a rubber cap at room temperature under nitrogen. A 75 μL sample of H_2O was injected by syringe into the tube. The tube was shaken and immediately transferred into the NMR probe. The reaction was followed by $^{31}P\{^1H\}$ and ^1H NMR spectroscopy at room temperature. All the starting β-chelates were converted into the binuclear compounds [Pd(μ-OH)(P-P)]$_2$(B(Ar′)$_4$)$_2$ (P-P = dmpf (**20**), depf (**21**), dippf (**22**)) and free 2-butanone with rates that increased in the order **17** ($t_{1/2}$ = 20 min) < **18** ($t_{1/2}$ = 7 min) < **19** ($t_{1/2}$ = 4 min). Some unidentified compounds (ca. 20%) were also observed in the final $^{31}P\{^1H\}$ NMR spectra. In parallel experiments, a 200 μL portion of the initial β-chelate solution was transferred by a syringe into an IR cell for liquids under nitrogen, and the reaction was followed by IR spectroscopy at room temperature (spectral range from 1500 to 1900 cm^{-1}). With time, the characteristic β-chelate band at ca. 1634 cm^{-1} decreased with formation of a new band at 1712 cm^{-1} due to 2-butanone, at a rate comparable to that observed in the NMR experiments (see Figure 4 for the dippf β-chelate **19**).

20. ^1H NMR (CD_2Cl_2): δ −1.45 (br s, μ-OH). $^{31}P\{^1H\}$ NMR (CD_2Cl_2): δ 22.1 (s).

21. ^1H NMR (CD_2Cl_2): δ −1.56 (br s, μ-OH). $^{31}P\{^1H\}$ NMR (CD_2Cl_2): δ 45.7 (s).

22. ^1H NMR (CD_2Cl_2): −2.34 (br s, μ-OH). $^{31}P\{^1H\}$ (CD_2Cl_2): δ 73.2 (s).

Copolymerization of CO and Ethylene. HPNMR Experiments with 4 as Catalyst Precursor. (A) MeOH-*d*$_4$. A 10 mm sapphire HPNMR tube was charged with a solution of **4** (10 mg, 0.013 mmol) in MeOH-*d*$_4$ (2 mL) under nitrogen and then placed into a NMR probe at 22 °C ($^{31}P\{^1H\}$ NMR singlet at δ 34.2). Pressurizing with a 1:1 mixture of CO and C_2H_4 to 20 bar at room temperature caused no change in both the ^1H and $^{31}P\{^1H\}$ NMR spectra. When the temperature was increased to 80 °C, the copolymerization reaction occurred. Compound **4** slowly disappeared with time, and formed in its place were several unidentified species. After 1 h, the tube was removed from the probe head. Similar NMR pictures were observed when an excess of BQ and/or TsOH was added to the reaction mixtures; the only difference was that the polymer appeared as a more brilliant off-white solid.

(B) D_2O. A 10 mm sapphire HPNMR tube was charged with a D_2O (2 mL) solution containing **4** (10 mg, 0.013 mmol) and a 10-fold excess of TsOH under nitrogen and then placed into a NMR probe at 22 °C ($^{31}P\{^1H\}$ NMR singlet at δ 32.2). Pressurizing with an 1:1 mixture of CO and C_2H_4 to 20 bar at room temperature caused no change in both the ^1H and $^{31}P\{^1H\}$ NMR spectra. Complex **4** was the only phosphorus-containing species visible by NMR also during the copolymerization reaction (1 h at 80 °C), although the intensity of its $^{31}P\{^1H\}$ NMR signal slowly decreased with time. The tube was then cooled to room temperature. A comparison between the $^{31}P\{^1H\}$ NMR spectrum of this sample and the spectrum acquired at room temperature before the catalytic reaction showed the concentration of **4** to decrease by ca. 35%.

Methoxycarbonylation of Ethylene. HPNMR Experiments with 6 as Catalyst Precursor in MeOH-d_4. The reaction was followed by variable-temperature $^{31}P\{^1H\}$ and ^1H NMR spectroscopy. A sequence of selected $^{31}P\{^1H\}$ NMR spectra is reported in Figure 3. A 10 mm sapphire HPNMR tube was charged under nitrogen with a solution of **6** (12 mg, 0.013 mmol) in MeOH-d_4 (2 mL) and then placed into the NMR probe at room temperature (δ 91.9, trace a). Pressurizing with a 1:1 mixture of CO/C_2H_4 to 40 bar at room temperature (trace b) led to the formation of two low-intensity doublets at δ 58.5 and 35.9 with a J(PP) value of 24 Hz, attributed to the β-chelate complexes [Pd($CH_2CH_2C(O)R$)(dippf)]OTs (**23**) on the basis of the spectrum of the authentic β-chelate **19**. The R group in **23** may be either $C_2H_4D(H)$ or OCD_3, depending on whether the reaction starts with Pd−D/H or Pd−OCD_3, respectively. Another minor species, marked by a broad $^{31}P\{^1H\}$ NMR signal at δ 34.5 (trace b), was assigned to the μ-hydrido μ-carbonyl complex [Pd_2(μ-H/D)(μ-CO)($dippf)_2$]OTs (**24H/D**; see the analogue **25H** below). The ^1H NMR spectrum contained a very weak signal at ca. δ −7 due to the μ-H hydrogen in **24H/D**, which suggests the involvement of the water molecules contained both in **6** and in the solvent in the formation of Pd−H moieties. Alternatively, the proton may come from H/D scrambling with ethylene via β-hydride elimination of palladium alkyl intermediates. Increasing the temperature, first to 50 °C and then to 80 °C (trace c), led to the quantitative conversion of **6** into **24H/D**, while the β-chelates **23** disappeared; some minor signals due to unknown species were also present. After 1 h at 80 °C, the probe head was cooled to room temperature. The β-chelate **23** reappeared in the $^{31}P\{^1H\}$ NMR spectrum (trace d). The tube was removed from the probe head; no solid material, except for traces of black palladium, was observed. The analysis of the solution by GC/MS showed the formation of deuterated samples of methyl propanoate and 3-pentanone.

In Situ Synthesis of [$Pd_2(\mu$-H)(μ-CO)($dippf)_2$]($B(Ar')_4)_2$ (25H). A 5 mm NMR tube was charged with a CD_2Cl_2 solution of [Pd(C(O)Me)(dippf)]B$(Ar')_4$ (**16**), prepared in situ by following a procedure analogous to those reported above. MeOH (10 equiv) was syringed into the solution in the presence of CO at room temperature. After ca. 1 h, ^1H and $^{31}P\{^1H\}$ NMR spectra showed the quantitative conversion of the starting acetyl complex ($^{31}P\{^1H\}$ NMR δ 15.4) into the binuclear species **25H** and methyl acetate.[11a] The solution was evaporated to dryness, and the residue was analyzed by IR spectroscopy (KBr, Nujol mull: ν(CO) 1825 cm^{-1}). When MeOH-d_4 was added to the solution of the starting acetyl complex, the deuterated analogue [$Pd_2(dippf)_2(\mu$-D)(μ-CO)]OTs (**25D**) was formed; three signals were observed in the $^{31}P\{^1H\}$ NMR spectrum in an intensity ratio of 1:1:1 due to the phosphorus−deuterium coupling (^2J(PD) = 5.9 Hz). $^{31}P\{^1H\}$ NMR (CH_2Cl_2): δ 33.6 (s). ^1H NMR (CH_2Cl_2): δ −7.14 (quintet, ^2J(HP) = 40.4 Hz, 1H, Pd−H), 1.3−1.6 (m, 24H, CH*Me*$_2$), 2.59 (m, 4H, C*H*Me$_2$), 4.42 (br s, 4H, β-H Cp), 4.52 (br s, 4H, β-H Cp), 4.68 (br s, 4H, α-H Cp), 4.82(d, 4H, α-H Cp).

Table 1. Crystal Data and Structure Refinement Details for 1 and 4

	1	4
empirical formula	$C_{29}H_{42}Cl_6Fe_2P_4Pd_2$	$C_{28}H_{36}FeO_7P_2PdS_2$
fw	1051.71	772.88
cryst color, shape	orange-red, block	deep red, prism
cryst size, mm	0.80 × 0.25 × 0.15	0.70 × 0.50 × 0.20
collection temp, K	293(2)	293(2)
cryst syst	monoclinic	monoclinic
space group	$P2_1$	$P2_1/n$
a, Å	12.618(4)	17.658(9)
b, Å	10.741(15)	9.783(3)
c, Å	14.354(8)	19.863(12)
β, deg	103.25	112.78(3)
V, Å^3	1894(3)	3164(3)
Z	2	4
calcd density, g/cm^3	1.845	1.623
F(000)	1044	1576
radiation/wavelength, Å	Mo Kα/0.710 73	Mo Kα/0.710 73
abs coeff, mm^{-1}	2.299	1.303
no. of rflns collected	3491	4335
no. of unique rflns	3491	4335
no. of data/restraints/params	3491/1/389	4335/0/378
goodness of fit on F^2	1.049	1.049
R1, wR2 ($I > 2\sigma(I)$)	0.0197, 0.0500	0.0327, 0.0782
R1, wR2 (all data)	0.0213, 0.0509	0.0532, 0.0857
largest diff peak and hole, e/Å^3	0.529, −0.345	0.677, −0.546

X-ray Data Collection and Structure Determination of 1 and 4. Diffraction data for both crystals were collected at room temperature on an Enraf-Nonius CAD4 automatic diffractometer with Mo Kα radiation (graphite monochromator). Unit cell parameters of both structures were determined from a least-squares refinement of the setting angles of 25 carefully centered reflections. Crystal data and data collection details are given in Table 1.

The intensities were rescaled and assigned a standard deviation $\sigma(I)$, calculated using the value of 0.03 for the instability factor k.[28] Lorentz−polarization and absorption corrections were applied.[29] Atomic scattering factors were taken from ref 30, and an anomalous dispersion correction, with real and imaginary parts, was applied.[31] The structures were solved by direct methods and refined by full-matrix F^2 refinement. All the calculations were performed on a PC using the WINGX package[32] with SIR-97,[33] SHELX-97,[34] and ORTEP-3[35] programs.

---

(28) Corfield, P. W. R.; Doedens, R. J.; Ibers, J. A. *Inorg. Chem.* **1967**, *6*, 197.

(29) Parkin, S.; Moezzi, B.; Hope, H. *J. Appl. Crystallogr.* **1995**, *28*, 53.

(30) Wilson, A. J. C. *International Tables for X-ray Crystallography*; Kluwer: Dordrecht, The Netherlands, 1992; p 500.

(31) Wilson, A. J. C. *International Tables for X-ray Crystallography*; Kluwer: Dordrecht, The Netherlands, 1992; p 219.

(32) Farrugia, L. J. *J. Appl. Crystallogr.* **1999**, *32*, 837.

(33) Altomare, A.; Burla, M. C.; Camalli, M.; Cascarano, G. L.; Giacovazzo, C.; Guagliardi, A.; Moliterni, A. G. G.; Polidori, G.; Spagna, R. *J. Appl. Crystallogr.* **1999**, *32*, 115.

(34) Sheldrick, G. M. SHELX97 Program for Crystal Structure Refinement; University of Göttingen, Göttingen, Germany, 1997.

(35) Burnett M. N.; Johnson, C. K. Report ORNL-6895; Oak Ridge National Laboratory, Oak Ridge, TN, 1996.

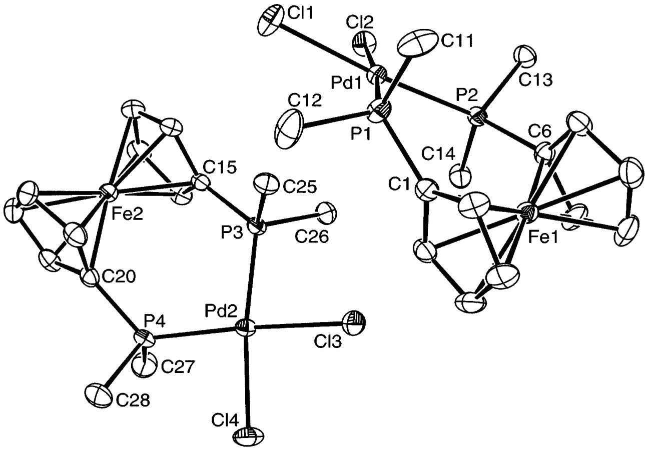

Figure 1. ORTEP drawings of the two conformers of 1 (**1a**, right; **1b**, left). Thermal ellipsoids are drawn at the 30% probability level. Hydrogen atoms have been omitted for clarity.

Results

Synthesis of the Catalyst Precursors. The Pd^{II} catalyst precursors employed in this study, namely [Pd(H_2O)(OTs)(dmpf)]OTs (**4**), [Pd(H_2O)(OTs)(depf)]OTs (**5**), and [Pd(H_2O)(OTs)(dippf)]OTs (**6**), were synthesized by reaction of the corresponding dichloride derivatives $PdCl_2$(P-P) (P-P = dmpf (**1**), depf (**2**), dippf (**3**)) with AgOTs in CH_2Cl_2, followed by precipitation with diethyl ether. Complexes **4**−**6** exhibit a fairly good solubility in water at 20 °C with concentrations as high as 48, 21, and 11 mg mL^{-1}, respectively. Just for comparison, the aryl-substituted complex [Pd(H_2O)(OTs)(dppf)]OTs (dppf = 1,1′-bis(diphenylphosphino)ferrocene) shows a much lower solubility of 0.15 mg mL^{-1}.

Multinuclear NMR spectroscopy (^{31}P, ^{1}H, ^{13}C) in either organic solvents (CD_2Cl_2, $CDCl_3$) or D_2O and conductivity measurements in nitroethane provided a reliable characterization for all compounds. On the basis of these studies all compounds were assigned a square-planar coordination around palladium, comprising a chelating diphosphine and a mutually cis tosylate anion and water molecule. A further authentication of the cis-chelating structures reported in Chart 1 was obtained by single-crystal X-ray analyses on the dmpf compounds **1** and **4**.

The crystal structure of **1** contains two different conformers (**a** and **b**) and one molecule of CH_2Cl_2 per asymmetric unit. Figure 1 shows an ORTEP drawing of the complex, while selected bond lengths and angles are listed in Table 2. The coordination geometry around the palladium atom can be described as slightly distorted square planar with cis-coordinating phosphorus atoms and is very similar to the geometries of $PdCl_2$(depf)[36] (**2**) and $PdCl_2$(dippf)[5b,10] (**3**). The values of the P−Pd−P angles in the conformers **1a** and **1b** are 99.64(9) and 98.95(9)°, respectively. These values are comparable to that found in **2** (97.74(3)°)[36] but significantly smaller than that in **3** (103.59(4)°).[5b,10] Unlike **3** and conformer **1b**, which show two identical (2.2941(9) Å) and almost identical Pd−P bond lengths (2.268(2) and 2.266(2) Å), respectively, conformer **1a** exhibits an unsymmetrical coordination of the phosphorus donor ligand (Pd(1)−P(1) = 2.256(2) Å, Pd(1)−P(2) = 2.280(2) Å). The tilting of the Cp rings, put in evidence by the angle between the plane normals of the sandwiching Cp rings, is in both conformers toward the palladium(II) center with values of 5.04 and 5.34°, respectively, which is comparable to the value of 3.70° for **3**.[10] The conformations of the Cp rings, described by the dihedral angles C(ipso)−$Cp_{centroid}$−$Cp_{centroid}$−C(ipso), are staggered (33.8 and 31.5°). Indeed, the values of the distortion angles of the Cp rings of both conformers are very close to that reported for **3** (32.5°).[10] The analysis of the short contacts within the crystal structure of **1** reveals the presence of eight short intermolecular distances between the chloride and hydrogen atoms (2.723−2.940 Å) and one short contact between H(11C) and H(2) of 2.254 Å.

From a perusal of the solid-state structures of the dichloride complexes **1**−**3** one may conclude that the three compounds exhibit similar coordination geometries, the only noticeable difference being the crystallographic bite angle P−Pd−P, which is larger in **3** as a consequence of the greater bulkiness of the *i*-Pr groups.

The crystal structure of **4** shows a square-planar monocationic compound where the metal atom is surrounded by a cis-chelating diphosphine, a tosylate anion, and a molecule of water. Figure 2 shows an ORTEP drawing of the complex cation, while selected bond lengths and angles are listed in Table 2.

The diphosphine forms a P(1)−Pd(1)−P(2) bite angle of 91.80(6)°, which is significantly smaller than that of the neutral dichloride precursor **1** (vide supra). The dihedral angle, defined as C(1)−Cp(1)−Cp(2)−C(6), of 16.20(1.25)° is similarly smaller than that in **1**. The angle between the plane normals related to the Cp rings is 3.57(0.76)° and is therefore comparable to those of the analogous dichloride species. Complex **4** exhibits two practically identical Pd−P bond lengths, as in the related complex [Pd(H_2O)(OTs)(dppp)]OTs (dppp = 1,3-bis(diphenylphosphino)propane).[37] The coordinated water molecule is involved in both intra- and intermolecular hydrogen bonds, with both coordinated and free tosylate anions, as evidenced by H···O distances of 1.938 and 1.891 Å, respectively.[13,37]

Catalytic Carbonylation of Ethylene and Ethylene/Propene. Complexes **4**−**6** were tested as catalyst precursors for the carbonylation of ethylene in MeOH and water or in a 1/1 mixture of water and 1,4-dioxane (hereafter referred to as DIOX). A preliminary NMR study showed all the precursors to be stable in these solvents for at least 2 h at room temperature.

The dmpf and depf complexes **4** and **5** were both active, yielding selectively alt-E-CO material, irrespective of the reaction solvent. In contrast, the dippf-modified precursor **6** gave exclusively low-molecular-weight oxygenates in MeOH, essentially diketones, keto esters, and diesters of the general formulas $Et(C(O)CH_2CH_2)_nH$ (n = 1−4), $MeO(C(O)CH_2CH_2)_nH$ (n = 1−4), and $MeO(C(O)CH_2CH_2)_nC(O)OMe$ (n = 1−4). Notably, the overall selectivity in EtC(O)Et and EtC(O)OMe was generally higher than 89%.

Initially, the reactions were performed under 40 bar of a 1/1 ethylene/CO mixture for 1 h at 85 °C with no

---

(36) Gusev, O. V.; Beletskaya, I. P. Manuscript in preparation.

(37) Benetollo, F.; Bertani, R.; Bombieri, G.; Toniolo, L. *Inorg. Chim. Acta* **1995**, *233*, 5.

Table 2. Selected Geometrical Parameters for 1 and 4

1a		**1b**		**4**	
		Bond Lengths (Å)			
Pd(1)−P(1)	2.256(2)	Pd(2)−P(3)	2.268(2)	Pd(1)−P(1)	2.235(1)
Pd(1)−P(2)	2.280(2)	Pd(2)−P(4)	2.266(2)	Pd(1)−P(2)	2.234(1)
Pd(1)−Cl(1)	2.368(3)	Pd(2)−Cl(3)	2.386(3)	Pd(1)−O(1)	2.123(4)
Pd(1)Cl(2)	2.368(2)	Pd(2)−Cl(4)	2.370(2)	Pd(1)−O(2)	2.131(3)
Pd(1)−Fe(1)	4.353(7)	Pd(2)−Fe(2)	4.390(7)	Pd(1)−Fe(1)	4.118(2)
Fe(1)−Cp(1)[a]	1.632(12)	Fe(1)−Cp(3)[a]	1.621(12)	Fe(1)−Cp(1)[a]	1.634(13)
Fe(1)−Cp(2)[a]	1.637(12)	Fe(1)−Cp(4)[a]	1.629(12)	Fe(1)−Cp(2)[a]	1.639(13)
		Bond Angles (deg)			
P(1)−Pd(1)−P(2)	99.64(9)	P(3)−Pd(2)−P(4)	98.95(9)	P(1)−Pd(1)−P(2)	91.80(6)
Cl(1)−Pd(1)−Cl(2)	88.89(10	Cl(3)−Pd(2)−Cl(4)	88.04(10)	O(1)−Pd(1)−O(2)	86.58(14)
P(1)−Pd(1)−Cl(2)	174.53(5)	P(3)−Pd(2)−Cl(4)	172.77(5)	O(1)−Pd(1)−P(1)	177.35(12)
		Dihedral and Pseudotorsion Angles (deg)			
C(1)Cp(1)Cp(2)C(6)[a]	33.81(1.10)	C(15)Cp(3)Cp(4)C(20)[a]	31.49(1.40)	C(1)Cp(1)Cp(2)C(6)[a]	16.20(1.25)
αCp[b]	5.04(0.50)	αCp[b]	5.34(0.80)	αCp[b]	3.57(0.76)
		Short Intermolecular Distances (Å)			
Cl(1)⋯H(11B)	2.881	Cl(2)⋯H(14C)	2.662		
Cl(1)⋯H(28B)	2.893	Cl(3)⋯H(19)	2.940		
Cl(2)⋯H(25C)	2.723	Cl(4)⋯H(29A)	2.737		
Cl(2)⋯H(9)	2.912	Cl(4)⋯H(13C)	2.781		
H(11C)⋯H(2)	2.254				
		Inter- and Intramolecular Hydrogen Lengths (Å) and Angles (deg)			
				H(1A)−O(5)	1.891
				H(1B)−O(4)	1.938
				O(1)−H(1B)−O(4)	158.33
				O(1)−H(1A)−O(5)	176.62

[a] Definitions: Cp(1), center of the C(1)−C(5) Cp ligand; Cp(2), center of the C(6)−C(10) Cp ligand; Cp(3), center of the C(15)−C(19) Cp ligand; Cp(4), center of the C(20)−C(24) Cp ligand. [b] Dihedral angle between the Cp planes.

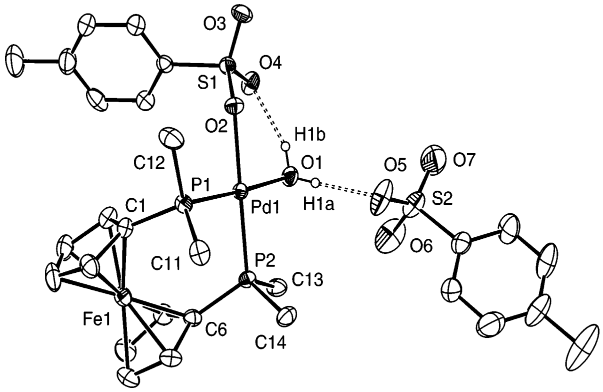

Figure 2. ORTEP drawing of **4**. Thermal ellipsoids are drawn at the 30% probability level. Hydrogen atoms have been omitted for clarity.

coreagent. Then, TsOH and BQ were added, separately or together, to the reaction mixtures using stoichiometries that are typical for alkene carbonylation catalyzed by diphosphine Pd^{II} complexes (20 equiv of TsOH and/or 80 equiv of BQ).[11,38] When appropriate, the catalytic activity was evaluated for a longer reaction time, generally 3 h. For the most active catalysts, experiments were carried out also at a lower pressure (20 bar) in an attempt to minimize mass transfer phenomena due to the fast filling up of the reactor by the insoluble copolymer.

The results of the reactions performed in MeOH are reported in Table 3. In the absence of coreagents, the dmpf precursor **4** was moderately active (entry 1), yet it showed a discrete stability (entries 1 and 2). A greater activity was obtained by adding either BQ (entry 3) or TsOH (entry 4). When they were added together, these coreagents improved the productivity up to 10.0 kg of product ((g of Pd) h)$^{-1}$ (entry 5). It may be worth noticing that this productivity is even larger than that obtained by the traditional Pd^{II} catalyst modified with the dppp ligand under the same reaction conditions (entry 21).[38c] A comparable productivity was obtained with the depf precursor **5**, even in the absence of coreagents (entry 8). By simply adding 80 equiv of BQ, the activity of **5** increased to 12.9 kg of product ((g of Pd) h)$^{-1}$ (entry 9). Interestingly, unlike **4**, no synergistic effect of the coreagents was observed with **5** (entry 12). The protic acid lowered the productivity, in fact (entry 8 vs entries 10 and 11). Reactions lasting 3 h showed the catalyst system generated by **5** to be rather stable both with no added coreagent (entries 13 and 14) and with BQ alone (entries 15 and 16).

Unlike the catalysts with the dmpf and depf precursors, the dippf complex **6** promoted the exclusive formation of low-molecular-weight oxygenates, irrespective of the experimental conditions (entries 17−20). The overall selectivity in EtC(O)Et and EtC(O)OMe was remarkably high, between 89 and 100%, and these products came out generally in a 1/1 ratio. In contrast, the turnover frequencies (TOFs) were rather modest, below 300 mol of ethylene incorporated ((mol of Pd) h)$^{-1}$.

In either water or DIOX solvents, only the dmpf and depf catalysts proved active for the carbonylation of ethylene and the presence of TsOH in the starting mixture was mandatory for high activity (Table 4). Indeed, no activity at all was observed without TsOH (entries 1, 6, and 15), while BQ alone did not significantly promote the carbonylation reaction (entries 2, 7, 12, and 16). The combined addition of BQ and TsOH

---

(38) (a) Bianchini, C.; Meli, A.; Müller, G.; Oberhauser, W.; Passaglia, E. *Organometallics* **2002**, *21*, 4965. (b) Bianchini, C.; Lee, H. M.; Meli, A.; Oberhauser, W.; Peruzzini, M.; Vizza, F. *Organometallics* **2002**, *21*, 16. (c) Bianchini, C.; Lee, H. M.; Meli, A.; Moneti, S.; Vizza, F.; Fontani, M.; Zanello, P. *Macromolecules* **1999**, *32*, 4183.

Table 3. Carbonylation of Ethylene Catalyzed by [Pd(OTs)(H_2O)(P-P)]OTs in MeOH[a]

						alt-E-CO					oligomers		
entry no.	P–P ligand	amt of BQ (equiv)	amt of TsOH (equiv)	CO/C_2H_4 pressure (bar)	time (h)	amt (g)	productivity[b]	TOF[c]	M_n (kg mol^{-1})	mp (°C)	EtC(O)OMe TOF[c]	EtC(O)Et TOF[c]	%[d]
1	dmpf	0	0	40	1	2.1	1.9	3 750	17.8	247			
2	dmpf	0	0	40	3	6.2	1.9	3 690					
3	dmpf	80	0	40	1	5.8	5.4	10 357					
4	dmpf	0	20	40	1	5.2	4.9	9 286					
5	dmpf	80	20	40	1	10.7	10.0	19 107	23.9	247			
6	dmpf	80	20	20	1	4.4	4.1	7 857					
7	dmpf	80	20	20	3	10.0	3.1	5 952					
8	depf	0	0	40	1	10.7	10.0	19 107	5.5	241			
9	depf	80	0	40	1	13.7	12.9	24 464	3.7	240			
10	depf	0	20	40	1	7.4	6.9	13 214					
11	depf	0	40	40	1	5.6	5.3	10 000					
12	depf	80	20	40	1	13.1	12.3	23 393					
13	depf	0	0	20	1	4.5	4.2	8 036					
14	depf	0	0	20	3	10.9	3.4	6 488					
15	depf	80	0	20	1	5.9	5.5	10 536					
16	depf	80	0	20	3	14.5	4.5	8 631					
17	dippf	0	0	40	1						35	25	100
18	dippf	80	0	40	1						135	74	94
19	dippf	0	20	40	1						282	277	89
20	dippf	80	20	40	1						165	149	93
21	dppp	80	20	40	1	8.0	7.5	14 276	22.7	248			

[a] Conditions: catalyst (0.01 mmol); MeOH (100 mL); 85 °C; 1400 rpm. [b] Productivity as kg of product ((g of Pd) h)$^{-1}$. [c] TOF as mol of ethylene incorporated ((mol of Pd) h)$^{-1}$. [d] Percentage of EtC(O)OMe + EtC(O)Et with respect to the overall oligomer production: Et(C(O)CH_2CH_2)$_n$H, $n = 1-4$; MeO(C(O)CH_2CH_2)$_n$H, $n = 1-4$; MeO(C(O)CH_2CH_2)$_n$C(O)OMe, $n = 1-4$.

Table 4. Carbonylation of Ethylene Catalyzed by [Pd(OTs)(H_2O)(P-P)]OTs in Aqueous Solvents[a]

						alt-E-CO				
entry no.	P–P ligand	solvent	amt of BQ (equiv)	amt of TsOH (equiv)	time (h)	g	productivity[b]	TOF[c]	M_n (kg mol^{-1})	mp (°C)
1	dmpf	DIOX[d]	0	0	1	0.0	0.0	0		
2	dmpf	DIOX	80	0	1	0.2	0.2	357		
3	dmpf	DIOX	0	20	1	3.5	3.3	6 250	20.8	242
4	dmpf	DIOX	80	20	1	3.8	3.6	6 786		
5	dmpf	DIOX	80	20	3	7.4	2.3	4 405		
6	dmpf	H_2O	0	0	1	0				
7	dmpf	H_2O	80	0	1	0				
8	dmpf	H_2O	0	20	1	0.2	0.2	357		
9	dmpf	H_2O	80	20	1	0.3	0.3	536		
10	dmpf	H_2O	80	20	3	0.6	0.2	357		
11	depf	DIOX	0	0	1	1.4	1.3	2 500		
12	depf	DIOX	80	0	1	1.6	1.5	2 857		
13	depf	DIOX	0	20	1	11.3	10.6	20 179	5.7	249
14	depf	DIOX	80	20	1	11.9	11.2	21 250		
15	depf	H_2O	0	0	1	0				
16	depf	H_2O	80	0	1	0				
17	depf	H_2O	0	20	1	0.7	0.7	1 250		
18	depf	H_2O	80	20	1	0.8	0.7	1 429		
19	depf	H_2O	80	20	3	2.0	0.6	1 190		

[a] Conditions: catalyst (0.01 mmol); solvent (100 mL); CO/C_2H_4 (40 bar); 85 °C; 1400 rpm. [b] Productivity as kg of product ((g of Pd) h)$^{-1}$. [c] TOF as mol of ethylene incorporated ((mol of Pd) h)$^{-1}$. [d] DIOX = 1/1 (v/v) H_2O/1,4-dioxane.

resulted in an almost negligible increase in productivity (entries 4, 9, 14, and 18).

Water alone was not a good solvent with either catalyst; just to make a comparison, the observed productivities were about 1 order of magnitude lower than those reported for other Pd^{II} catalysts modified with water-soluble chelating diphosphines such as Na_2-DPPPDS[39] ((NaO$_3$S(C_6H_4)CH_2)$_2$C(CH_2PPh$_2$)$_2$) and DPPPr-S[40] (1,3-C_3H_6(P(C_6H_4-m-SO$_3$Na)$_2$)$_2$). However, the activity of the depf catalyst was found to increase remarkably in DIOX, up to 11.2 kg of product ((g of Pd) h)$^{-1}$ (entry 14), which is comparable to the highest productivity obtained with the same catalyst in MeOH (Table 3, entries 9 and 12) and higher than those reported for both Na_2DPPPDS and DPPPr-S palladium(II) catalysts.[39,40]

The number-average molecular weight (M_n) (determined by ^{1}H NMR) of the alt-E-CO materials was found to depend on the catalyst rather than on the experimental conditions. M_n values between 3 and 6 kg mol^{-1} were obtained with the depf precursor, while the dmpf complex gave products with M_n values in the range 17–24 kg mol^{-1}. The melting points of all materials (240–250 °C) were comparable to those of copolymers commonly produced with chelating diphosphine ligands (see Table 3, entry 21, for instance). Keto and ester end groups in a 1/1 ratio were observed by NMR spectroscopy for the alt-E-CO materials produced in MeOH,

---

(39) Bianchini, C.; Lee, H. M.; Meli, A.; Moneti, S.; Patinec, V.; Pretrucci, G.; Vizza, F. *Macromolecules* **1999**, *32*, 3859.

(40) (a) Verspui, G.; Schanssema, F.; Sheldon, R. A. *Appl. Catal.* **2000**, *198*, 5. (b) Verspui, G.; Schanssema, F.; Sheldon, R. A. *Angew. Chem., Int. Ed.* **2000**, *39*, 804.

Table 5. Terpolymerization of Carbon Monoxide with Ethene/Propene Catalyzed by [Pd(OTs)(H_2O)(P-P)]OTs[a]

						alt-E/P−CO				
entry no.	P−P ligand	solvent	amt of BQ (equiv)	amt of TsOH (equiv)	amt of propene (g)	amt (g)	productivity[b]	propene (%)[c]	M_n (kg mol^{-1})	mp (°C)
1	dmpf	MeOH	80	20	3.6	5.0	4.7	2.1	10.8	236
2	dmpf	MeOH	80	20	9.4	6.8	6.4	5.8	6.7	221
3	dmpf	MeOH	80	20	14.0	7.5	7.0	9.9	6.2	220
4	dmpf	DIOX[d]	0	20	3.4	3.4	3.2	4.1	8.2	225
5	dmpf	DIOX	0	20	7.0	5.9	5.5	8.2	8.3	211
6	depf	MeOH	80	0	4.0	12.2	11.5	3.4	4.9	231
7	depf	MeOH	80	0	11.4	6.0	5.6	15.6	3.9	195
8	depf	DIOX	0	20	3.4	6.5	6.1	3.4	3.3	228
9	depf	DIOX	0	20	6.6	6.3	5.9	11.4	3.2	199
10	dppp[e]	MeOH	80	20	20.0	17.0	5.3	6.0	14.1	224

[a] Conditions: catalyst (0.01 mmol); solvent (100 mL); CO/C_2H_4 (40 bar); 85 °C; 1 h; 1400 rpm. [b] Productivity as kg of product ((g of Pd) h)$^{-1}$. [c] Amount of propene incorporated in the polymeric chains as calculated by ^{1}H NMR integration. [d] DIOX = 1/1 (v/v) H_2O/1,4-dioxane. [e] Conditions: catalyst (0.01 mmol); MeOH (100 mL); CO/C_2H_4 (40 bar); 85 °C; 3 h; 1400 rpm.[38b]

whereas only keto end groups featured the polyketones obtained in aqueous solvents.[39,40]

The dmpf and depf precursors **4** and **5** were able to generate active catalysts also for the terpolymerization of CO with ethylene and propene in either MeOH or DIOX (Table 5). The incorporation of propene into the polymer chains was high enough with either catalyst (up to 16% with respect to ethylene) to obtain a significant modulation of the polymer properties. Indeed, some terpolymers showed melting points as low as 199 °C with a decrease of ca. 50 °C as compared to the copolymers. Surprisingly, the productivity in terpolymer obtained with the dmpf catalyst increased with the initial amount of propene (entries 1−3 in MeOH and entries 4 and 5 in DIOX).

As was observed for the copolymers, the M_n values of the terpolymers obtained with the dmpf were higher than those of the materials produced by the depf catalyst. The NMR analysis of the terpolymers showed the presence of keto and ester end groups in a ca. 1/1 ratio for the materials obtained in MeOH and of keto groups only for the materials obtained in aqueous solvents. The ^{13}C NMR signals due to the $-CH_2C(O)CH(Me)CH_2-$ and $-CH_2(CO)CH_2CH(Me)-$ units were in a ca. 1/1 ratio, thus indicating a comparable preference for both 1,2- and 2,1-insertion of propene into the propagating Pd−C(O)R.

The TGA analysis of the copolymers and terpolymers showed all the products to degrade around 262−270 °C, which is likely due to the presence of more than 15 ppm of residual palladium in the materials.[41,43] It is well-known, in fact, that the residual palladium may promote intra- and intermolecular dehydration reactions of polyketones with formation of both cross-links and heterocyclic compounds.[42]

The DSC analysis showed the occurrence of at least two different types of endothermic transitions. The less intense endotherm was observed at about 70−110 °C and was attributed to the transition from the α to the β phase, typical for alt-E-CO materials,[43] while the higher temperature transition (from 160 to 270 °C) was safely assigned to the melting peaks. From a comparison of the enthalpy values associated to the α/β transition (when detectable), one may infer that the α content decreases by increasing the incorporation of propene in the polymer backbone.[44] The melting transition of the terpolymers was characterized by a broad peak consisting of two or three melting points (maximum of peaks);[43] the temperature and the enthalpy associated with the melting decreased by increasing the amount of propene.[45] In both copolymers and terpolymers, lower melting transition temperatures and enthalpy values were observed in the second scan after cooling to room temperature, which has been attributed to extensive degradation on the basis of DSC measurements performed in different temperature intervals and at slow cooling rates.[43]

The straightforward copolymerization of CO with propene was attempted several times under different experimental conditions. In all cases, however, both **4** and **5** produced oligomers in very low yield.

Operando HPNMR Study of the Carbonylation of Ethylene Catalyzed by 4−6. A ^{1}H and ^{31}P{^{1}H} HPNMR study[38,39] of the reactions catalyzed by the precursors **4** and **5** in MeOH-d_4 and D_2O did not provide any useful information on either intermediates or resting states. Instead, β-chelate species **23** were unambiguously detected along the methoxycarbonylation of ethylene catalyzed by **6** (Figure 3).

β-Chelates are typical resting states of ethylene carbonylation by Pd^{II}-chelating diphosphine catalysis, and their presence in the reactions catalyzed by **6** accounts well for the observed formation of EtC(O)Et and EtC(O)OMe. Authentication of the β-chelates was provided by the synthesis and characterization of the model complex [Pd($CH_2CH_2C(O)Me$)(dippf)]B(Ar′)$_4$ (**19**; see below).

Besides β-chelates, the HPNMR spectra showed the formation and persistent presence of the μ-hydrido μ-carbonyl complex [Pd$_2$(μ-H/D)(μ-CO)(dippf)$_2$]OTs (**20H/D**).[11] This binuclear complex is a typical end product/resting state of ethylene carbonylation by Pd^{II}-chelating diphosphine catalysis, especially with ferrocenyldiphosphine ligands. Its formation has been proved to involve the condensation Pd^{II}−H species with Pd^0(CO) species, as illustrated in Scheme 2 for a generic ferrocenyldiphoshine complex.

---

(41) DeVito, S.; Bronco, S. *Polym. Degrad. Stab.* **1999**, *63*, 399.
(42) Lommerts, B. J. *Polymer* **2001**, *42*, 6283.
(43) Sommazzi, A.; Garbassi, F. *Prog. Polym. Sci.* **1997**, *22*, 1547.
(44) Lagaron, J. M.; Vickers, M. E.; Powell, A. K.; Davidson, N. S. *Polymer* **2000**, *41*, 3011.
(45) Lagaron, J. M.; Vickers, M. E.; Powell, A. K.; Bonner, J. G.. *Polymer* **2002**, *43*, 1877.

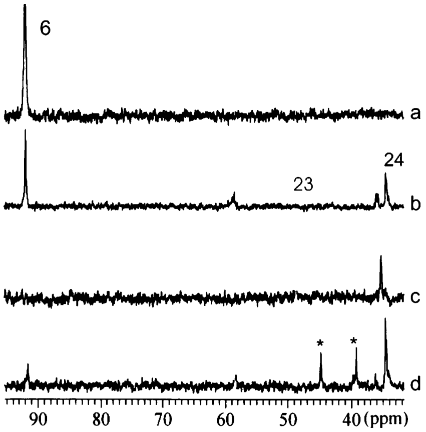

Figure 3. Variable-temperature $^{31}P\{^1H\}$ NMR study (sapphire tube, MeOH-d_4, 81.01 MHz) of the carbonylation reaction of ethylene catalyzed by **6**: (a) dissolving **6** in MeOH-d_4 under nitrogen at room temperature; (b) after the tube was pressurized with 40 bar of (1/1) CO/C_2H_4 at room temperature; (c) at 80 °C; (d) after the tube was cooled to room temperature. Asterisks denote unknown species.

Scheme 2

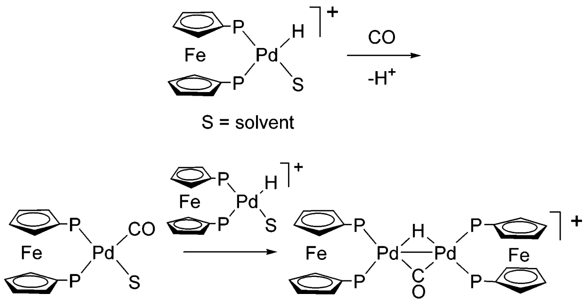

In Situ HPNMR and IR Studies of the Protonolysis of the β-Chelates [Pd(CH₂CH₂C(O)Me)(P−P)]B(Ar′)₄. The β-chelates **17**−**19** were prepared through a well-known synthetic protocol that involves, as the final step, the reaction of ethylene with the acetyl derivatives **14**−**16** (Scheme 3).

The reaction of Pd^{II} β-chelates with water is currently used to mimic the chain transfer of CO/ethylene copolymerization by protonolysis and, when followed by NMR spectroscopy, provides a reliable method to estimate the termination rate. In the dashed box of Scheme 3 is illustrated the protonolysis mechanism of the β-chelates as demonstrated by van Leeuwen. Therefore, an H_2O sample (25 μL per 0.01 mmol) was syringed into an NMR tube containing a CD_2Cl_2 solution of the appropriate β-chelate complex. As expected, all compounds were transformed at room temperature into the binuclear complexes $[Pd(\mu\text{-}OH)(P\text{-}P)]_2(B(Ar')_4)_2$ (P-P = dmpf (**20**), depf (**21**), dippf (**22**)) with formation of free 2-butanone. The transformation rates increased in the order **17** ($t_{1/2}$ = 20 min) < **18** ($t_{1/2}$ = 7 min) < **19** ($t_{1/2}$ = 4 min). The same order was found when the protonolysis reactions were monitored by IR spectroscopy in CH_2Cl_2, looking at both the disappearance of the β-chelate ν(CO) band and the concomitant formation of 2-butanone (ν(C=O) at 1712 cm^{-1}). Figure 4 shows some sequential spectra relative to the protonolysis of **19** (ν(CO) band at 1634 cm^{-1}).

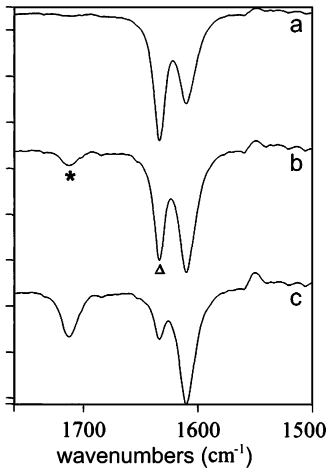

Figure 4. IR study of the reaction of **19** with water (CH_2Cl_2, room temperature): (a) addition of water; (b) after 15 min; (c) after 30 min. The asterisk denotes ν(C=O) at 1712 cm^{-1} of 2-butanone, and the open triangle denotes ν(C=O) at 1634 cm^{-1} of **19**.

The faster protonolysis of the β-chelate **18** as compared to **17** is apparently consistent with the lower molecular weight of the alt-E-CO material obtained with the depf precursor **5** (Table 3, entries 8 and 9 vs entries 1 and 5).

Discussion

In this work, we have examined the catalytic behavior of Pd^{II} complexes modified with ferrocenyldiphosphine

Scheme 3

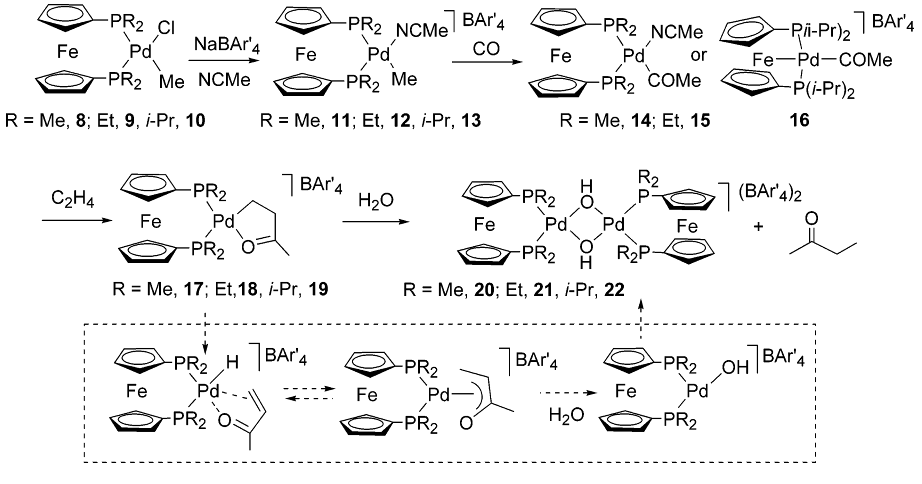

Scheme 4

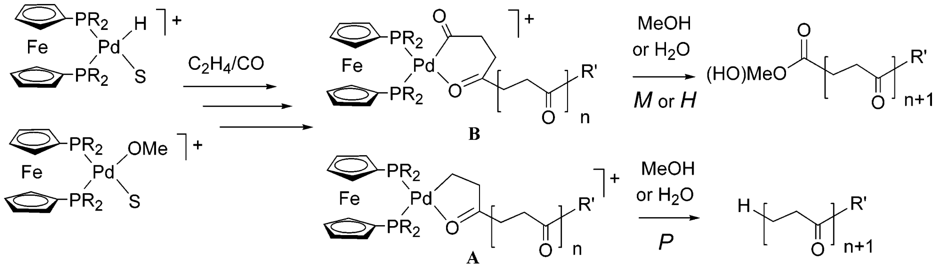

ligands bearing methyl, ethyl, and isopropyl substituents on the phosphorus atoms. The principal results obtained may be summarized as follows. (i) Irrespective of the solvent, the dmpf and depf complexes generate selective catalysts for the production of alt-E-CO copolymers and terpolymers. (ii) The dmpf catalyst is highly active in MeOH in the presence of both BQ and TsOH. (iii) The depf catalyst is highly active in MeOH even in the absence of oxidant or protic acid, whereas, in aqueous solvents, the presence of TsOH is required to maintain high activity. (iv) The dippf complex is an active catalyst only in MeOH, where EtC(O)Et and EtC(O)OMe are selectively produced. (iii) The chemical stability of all catalysts under methoxycarbonylation conditions is generally high, even in the absence of added oxidant or protic acid.

For a better comprehension of the results obtained, especially in an attempt to rationalize structure−activity relationships, it may be useful to recall the behavior of the prototypical ligand dppf. In conjunction with Pd^{II}, this ligand forms a poorly selective catalyst for the carbonylation of ethylene in MeOH, yielding all the compounds shown in Scheme 1.[11] Moreover, its low chemical stability under methoxycarbonylation conditions does not allow one to extend the reaction time above 1 h, which apparently limits the overall productivity. The overall TOFs under experimental conditions comparable to those adopted in this work (MeOH, 30 bar of 1/1 CO/C_2H_4, 85 °C) are as follows: 1376 (with neither BQ nor TsOH), 6143 (with 20 equiv of TsOH), 5464 (with 20 equiv of TsOH and 80 equiv of BQ).[11]

The dmpf and depf catalysts are much more stable and productive than the dppf analogue, which can be ascribed to the greater basicity of the alkyl-substituted ligands (dppf $\ll$ dmpf < depf < dippf).[21] Cyclic voltammetric studies have shown, in fact, that the reduction potential of Pd^{II} ferrocenyldiphosphine complexes becomes more negative as the basicity of the phosphorus donors increases.[11,46] Electron-rich phosphorus ligands would therefore disfavor the degradation of Pd^{II}(diphosphine) catalysts that is essentially due to the reduction of Pd^{II} to Pd^0. For this reason, the CO−ethylene copolymerization reactions generally provide higher productivities when carried out in the presence of oxidants, such as BQ, and protic acids.[11,38a,b,39,40]

On the basis of both catalytic and model studies, there is no reason to exclude the noiton that the present dmpf and depf catalysts copolymerize CO and ethylene via a well-established mechanism, whose main steps are illustrated in Scheme 4. Details of the catalytic cycles together with kinetic data may be found in the relevant literature.[22,43,47] It suffices here to say that, with either Pd−H or Pd−OMe initiators as the starting material, the alternating addition of ethylene/CO can proceed via β-chelate (**A**) or γ-chelate (**B**) propagating species that often are rate-limiting steps. The chain transfer can occur by either methanolysis (*M*)/hydrolysis (*H*) of Pd−acyl or protonolysis (*P*) of Pd−alkyl. Which of the two initiation and termination steps prevails depends on many factors, such as the specific catalyst, solvent, acid, or oxidant concentration.[22,47]

The absence of acid end groups (−COOH) in the alt-E-CO copolymers and terpolymers obtained from the aqueous reactions (Tables 4 and 5) suggests that the chain transfer occurs predominantly, if not exclusively, by protonolysis (Scheme 4, path *P*). Whether protonolysis is the predominant chain-transfer mechanism also in MeOH is hard to assess on the basis of the chain-end analysis, as the polyketones obtained in MeOH contain ester and ketone end groups in a ca. 1/1 ratio.

Another point that would deserve a further investigation pertains to the molecular weights M_n of the polyketones, which are higher with the dmpf catalyst (17−24 kg mol^{-1}) than with the depf catalyst (3−6 kg mol^{-1}). In this case, steric effects should prevail over electronic effects. In particular, it is possible that the bulkier ethyl substituents favor the termination by both protonolysis (destabilizing the propagating β-chelates, see the in situ IR and HPNMR studies) and methanolysis.[11a,18c,48]

Surprisingly, the productivity in terpolymer obtained with the dmpf catalyst has been found to increase with the initial amount of propene (Table 5, entries 1−3 in MeOH and entries 4 and 5 in DIOX). This finding is in contrast with both the present data with depf and previous reports, as the copresence of propene commonly shortens the polyketone chains and also reduces the overall productivity. Indeed, by favoring chain transfer over chain propagation, the frequency of formation of unstable Pd−H moieties would increase, thus accelerating catalyst degradation.

The increased productivity of the terpolymerization reaction catalyzed by **4** is somehow reminiscent of the so-called “comonomer effect” that is often encountered in copolymerization reactions of ethylene with α-olefins by metallocene or late-transition-metal catalysis.[49] The “comonomer effect” has still not been unraveled mecha-

---

(46) Gusev, O. V.; Peterleitner, M. G.; Vologdin, N. V.; Kal’sin, A. M. *Electrochemistry* **2003**, 39, 1444.

(47) (a) Sen, A. *Acc. Chem. Res.* **1993**, *26*, 303. (b) Drent, E.; Budzelaar, P. H. M. *Chem. Rev.* **1996**, *96*, 663. (c) Robertson, R. A. M.; Cole-Hamilton, D. J. *Coord. Chem. Rev.* **2002**, *225*, 67. (d) Bianchini, C.; Meli, A.; Oberhauser, W. *Dalton* **2003**, *2627*.

(48) Liu, J.; Heaton, B. T.; Iggo, J. A.; Whyman, R. *Chem. Commun.* **2004**, 1326.

(49) (a) Spitz, R.; Duranel, L.; Masson, P.; Darricades-Llauro, M. F.; Giyot, A. In *Transition Metal Catalyzed Polymerizations*; Quirk, R. P., Ed.; Cambridge University Press: Cambridge, U.K., 1988; p 719. (b) Herfert, N.; Montag, P.; Fink, G. *Makromol. Chem.* **1993**, *194*, 3167.

Scheme 5

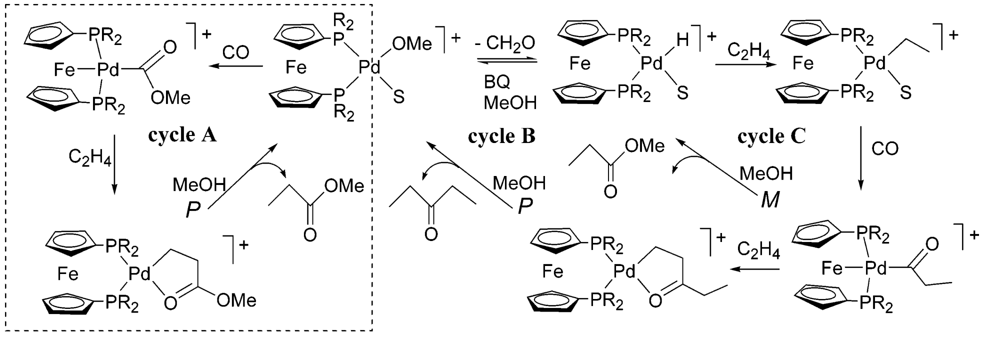

R = *i*-Pr S = MeOH, monomer *P* = protonolysis *M* = methanolysis

Chart 3

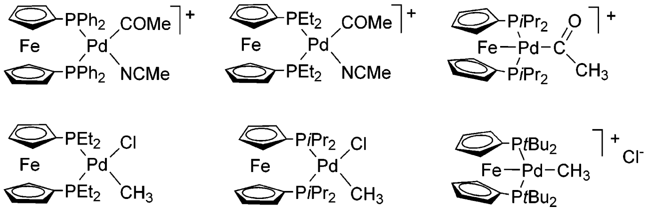

Scheme 6

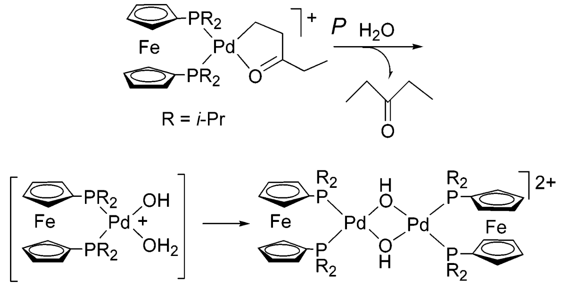

nistically, and the most common interpretation is that the addition of the α-olefin wakes "sleeping metal centers" in ethylene homopolymerization.[49] In the present terpolymerization reaction, it is possible that propene is more effective than ethylene for the stabilization of either Pd^{II}−H or Pd^0 intermediates (Scheme 2). Once coordinated to palladium, propene can either insert into Pd−H or be displaced by ethylene. In this picture, the coordination of propene might be facilitated by the (diphosphino)ferrocenyl ligand with the smallest substituents at phosphorus: i.e., dmpf.

If the higher basicity of dmpf and depf as compared to dppf is the key factor accounting for the higher productivity exhibited by **4** and **5**, the basicity of the phosphorus donors cannot explain why the dippf-modified catalyst derived from **6** is much less active and, most importantly, selective for methyl propanoate and 3-pentanone. Steric effects apparently play a major role in determining the catalytic activity of **6**. As shown in Chart 3, the phenyl substituents[18a] as well as the ethyl ones allow the phosphorus atoms to be mutually cis in the acetyl complexes $[Pd(NCMe)(C(O)Me)(P\text{-}P)]^+$ (P-P = dppf, depf), whereas the *i*-Pr groups favor the κ^3-*P,P,Fe* bonding mode.[18a,c] In the case of coligands with no electron-withdrawing character such as the methyl group, the bulkier *t*-Bu groups are required for the trans disposition of the phosphorus atoms.[18b] The formation of the κ^3-*P,P,Fe* bonding mode is actually favored by electron-withdrawing coligands (−C(O)R and −C(O)OR, for instance) that make palladium(II) more suitable to receive the iron-centered e_{2g} electron density.[3,11a,13,18]

Just the formation of a dative Fe−Pd bond, especially in the acyl and carboalkoxy complexes, may be the factor that makes the dippf catalyst selective for methyl propanoate and 3-pentanone. Scheme 5 shows the possible pathways for the production of the latter products.

Methyl propanoate can be obtained either by protonolysis of the β-chelate bearing the ester group (cycle A, dashed box) or by methanolysis of the Pd-propionyl complex (cycle C). The former cycle is probably less important than cycle C. Indeed, the addition of BQ, which increases the concentration of Pd−OMe in the catalytic mixtures,[22,47b] yields less methyl propanoate than the reaction performed in the presence of TsOH alone (Table 3, entry 18 vs entry 19). The stability of the κ^3-*P,P,Fe* carboalkoxy intermediate to ethylene insertion may contribute to the sluggishness of cycle A.[11a] Indeed, the insertion of ethylene requires a free coordination site cis to the ester group and cis phosphorus atoms. This process is apparently difficult to accomplish, due to the electron-withdrawing character of the ester ligand that strengthens the Fe−Pd bond, favoring a trans disposition of the phosphorus atoms.

3-Pentanone is exclusively produced in cycle B by protonolysis of the keto β-chelate. Since methyl propanoate and 3-pentanone are obtained with comparable TOFs (Table 3, entries 17−20), one may conclude that the reactions of the κ^3-*P,P,Fe* acyl intermediate with either MeOH (methanolysis) or ethylene (migratory insertion) occur at a comparable rate. This suggests that the step limiting both rates is just the hapticity change of dippf from κ^3-*P,P,Fe* to κ^2-*P,P,* because both the methanolysis of the propionyl complex and the formation of the β-chelate require *cis*-P atoms to occur.[18c,48]

The overall selectivity of **6** in methyl propanoate and 3-pentanone shows unequivocally that the protonolysis of the keto β-chelate in cycle **B** is much faster than the uptake of CO to give the next γ-chelate (see Scheme 4). The very fast protonolysis of the first β-chelate (see the in situ IR and HPNMR studies) can also contribute to make the dippf precursor **6** inactive in aqueous solvents. Indeed, the catalytic reaction would immediately stop by incorporation of active palladium(II) into an inactive μ-OH binuclear complex (Scheme 6).

To the best of our knowledge, **6** is the only bis(diorganylphosphino)ferrocenyl Pd^{II} complex capable of producing significant amounts of 3-pentanone in ethylene methoxycarbonylation reactions. In fact, all the other known catalysts for low-molecular-weight oxygenates give predominantly methyl propanoate.[3,11,47c]

Conclusions

Palladium(II) complexes of the formula [Pd(H_2O)(OTs){1,1′-bis(dialkylphosphino)ferrocene}]OTs (alkyl = Me, Et, *i*-Pr) are active catalysts for the carbonylation of ethylene in MeOH, water, or a water/1,4-dioxane mixture. It has been found that the catalytic activity is affected by both electronic and steric effects induced by the ferrocenyldiphosphine ligands. Electronic effects play a major role in controlling the productivity in either alternating CO−ethylene copolymers or CO−ethylene−propene terpolymers, while steric effects are crucial in driving the selectivity toward either alt-E-CO materials or the single-carbonylation products methyl propanoate and 3-pentanone. The macromolecular properties of the polyketones can be tuned by an appropriate choice either of the metallocene ligands or of the reaction medium.

Acknowledgment. Thanks are due to the European Commission (Contract HPRN-CT-2002-00196, PALLADIUM project), the Russian Foundation for Basic Research (Grant 03-03-32471), and the Science Support Foundation of the Russian Federation for financial support.

Supporting Information Available: TGA and DSC data of selected polymers (Table 1S and Figure 1S) and text and tables giving crystallographic data for compounds **1** and **4**. This material is available free of charge via the Internet at http://pubs.acs.org.

OM049109W